

Required number of states increases only moderately with the problem size for antisymmetrized geminal powers

Wataru Uemura and Takahito Nakajima

RIKEN Center for Computational Science, Kobe 650-0047, Japan

We propose an algorithm to obtain the ground-state energy of a many-electron system using the variational wave function of a linear combination of antisymmetrized geminal powers. We optimized this algorithm to obtain the energy and the other parameters of a many-electron system. Also we clarified the bottleneck of the total calculation in the tensor contraction and successfully reduced the computational time. As a result, we can use an extended number of geminal states to obtain the ground state of the water molecule and Hubbard models. The result for the water molecule with the Dunning double-zeta basis is of the sub-millihartree order above the energy of exact diagonalization. Further, we observe that the result for the one-dimensional Hubbard model with 14 sites shows good tendency to capture the right ground state and that for the two-dimensional Hubbard model still lacks some part of the energy reflecting the large size of the Hilbert space. We conclude that the required number of terms for geminal states for sufficiently accurate energy is only moderately affected by the problem size. We further show other technical details for the numerical algorithms of geminal states in the variation process. It is expected that with the use of more extended computing resources and larger sizes of electronic systems, our algorithm can provide improved results.

I. INTRODUCTION

The many-electron problem in quantum chemistry or quantum lattice models is still considered as an important subject of modern science. With the growth of large-scale computer facilities, it has become possible to not only solve these problems with the exact diagonalization but also construct numerical algorithms that could handle the complex behaviors of electronic correlation.

In post-Hartree-Fock theories, perhaps the most simple and convenient method is configuration interaction.[1, 2] Configuration interaction is built on the basis of the Hartree-Fock theory, and a small or large number of configurations are chosen for each approximation level. Obtaining energy results of high precision is limited by the large scaling problem of the algorithm.

The configuration interaction or coupled cluster[3] is regarded as a single reference that is based on the results of one Hartree-Fock configuration. There is already an established framework for multi-reference configuration interaction (MRCI).[4] MRCI uses several configurations for the building blocks and applies excitation or other operators to these configurations. Thus, the MRCI can obtain results that are very close to the exact result; however, the calculations become prohibitively expensive for large molecules. The multi-reference coupled cluster (MRCC) is also used in such applications, but it is yet early to provide any systematic applications.[5, 6]

In the area of macroscopic materials, the most successful method for the many-electron problem is density functional theory (DFT).[7–9] The formalism of DFT is based on the assumption that there is a one-to-one correspondence between the total wave function and the single-electron density. The Kohn-Sham equation is built on this theory and treats the system on the basis of the Hartree-Fock theory. If we can replace the Hartree-Fock strategy in DFT with a more sophisticated one with

multi-reference wavefunction ansatz, then we can possibly obtain a large part of the correlation energy of the target system.

When solving the many-electron problem with multi-reference theory, quantum Monte Carlo (QMC) is a highly reliable tool.[10–20] It is common to combine the Slater determinant with the Jastrow factor to obtain the solution of a target system. In some cases, the wavefunction is extended to use the Pfaffian or antisymmetrized geminal power (AGP) states to obtain an accurate ground state. There are known problems in QMC; it suffers from the well-known negative-sign problem with the usage of probability.

The formalism of configuration interaction or MRCI is not dependent on the probability and is instead based on a discrete set of configurations. If we construct the Slater determinants from continuous matrices, the degree of freedom for the variation is extended considerably. On this subject, there are foregoing research works mainly on Hubbard models.[21–24] The formalism of their calculations is based on the evaluation of the matrix element of the overlap of the multi-Slater determinant with matrices representing the orbitals on each site. Because of the nature of the Hubbard model that has a simple form of the correlation term, the calculation for Hubbard models with non-orthogonal determinants could be achieved with low computational scaling. With this formalism, the ground states of one-dimensional and two-dimensional Hubbard models are captured adequately and with good precision of the energy. Recently, new results have been reported that are aided by large computing facilities.[25–27] These report highly accurate results with the consideration of the spin and spatial symmetry for the Hubbard model as well as qualitatively good results for the selected molecular systems.

The electronic states of the Slater determinants are classified as non-interacting, and they are described by rectangular matrices and their inverse matrices. There

are suggestions in the context of reduced density matrices for the fermionic system to use the antisymmetrized geminal power states instead of the Slater determinants.[28–34] We have recently shown the formula for the density matrices for geminal states and variational calculations with the superpositions of geminal states.[35, 36] The result were, in some cases, highly accurate when compared with the exact diagonalization. An algorithm was included to avoid the divergent-like behavior of the AGP energy. We have extended the number of states for the AGP and tested the same molecular system and the Hubbard model with increased number of electrons. The results are especially accurate in the case of a moderate number of geminal states. From these observations, we concluded that the exact ground-state wavefunction could be described with a moderate number of states for multi-reference AGP ansatz. In the next section, we provide some algorithms for the energy variation of the AGP states.

II. FORMALISM

First, we introduce the derivation of the expression for energy with two AGP states. This result was first indicated in ref.[35]. When constructing the AGP state from matrix parameters, we use the permutation tensor

$$\epsilon_{i_1 \dots i_N} = \hat{A}(\epsilon_{i_1 i_2} \epsilon_{i_3 i_4} \dots \epsilon_{i_{N-1} i_N}). \quad (1)$$

The matrix ϵ is defined in ref.[35] as a skew-symmetric matrix. From the permutation tensor, we can construct the AGP wavefunction as

$$A_{i_1 \dots i_N} = \sum_{k_1 \dots k_N} \epsilon_{k_1 \dots k_N} \alpha_{k_1 i_1} \dots \alpha_{k_N i_N}. \quad (2)$$

Here, α is a general matrix. We also define the superposition of the AGP states as

$$A_{i_1 \dots i_N} = \sum_{k=1}^K c_k \sum_{k_1 \dots k_N} \epsilon_{k_1 \dots k_N} \alpha_{k_1 i_1}^k \dots \alpha_{k_N i_N}^k, \quad (3)$$

where c_k is a variational parameter. This representation with α is equivalent to the AGP states with geminal γ by the relationship

$$\gamma_{i_1 i_2} = \sum_{k_1 k_2} \epsilon_{k_1 k_2} \alpha_{k_1 i_1} \alpha_{k_2 i_2}. \quad (4)$$

From matrix α , we can construct the overlap of the AGP state as

$$n = \sum_{i_1 \dots i_N j_1 \dots j_N} \epsilon_{i_1 \dots i_N} \epsilon_{j_1 \dots j_N} a_{i_1 j_1} \dots a_{i_N j_N}, \quad (5)$$

where

$$a = \alpha^t \alpha. \quad (6)$$

Expression ${}^t x$ shows the matrix transpose of matrix x . When we substitute the permutation tensor ϵ of eq.(1) in eq.(5), we can obtain the explicit formula for the AGP norm as

$$n = 3(\text{tr } A)^2 - 6(\text{tr } A^2) \quad (7)$$

for $N = 4$, and

$$n = 15(\text{tr } A)^3 - 90(\text{tr } A)(\text{tr } A^2) + 120(\text{tr } A^3) \quad (8)$$

for $N = 6$. Here, matrix A is defined as

$$A = a \epsilon^t a^t \epsilon. \quad (9)$$

These equations are similar to the ones that are obtained in the context of nuclear physics.[37] We can obtain the general result as

$$n = N! \exp\left(\frac{1}{2} \text{tr} \log(1 + At)\right)|_{t^{N/2}} \quad (10)$$

$$\equiv N! \text{pf}(1 + At)|_{t^{N/2}}, \quad (11)$$

which is equivalent to the norm expression given in ref.[35]. The subscript $t^{N/2}$ represents the $N/2$ -order coefficient of t .

Next, we introduce the method to obtain the second-order reduced density matrix for the AGP state. We can use the second derivative of the norm as

$$\begin{aligned} & \frac{\partial}{\partial a_{k_1 l_1}} \frac{\partial}{\partial a_{k_2 l_2}} \sum_{i_1 \dots i_N j_1 \dots j_N} a_{i_1 j_1} \dots a_{i_N j_N} \epsilon_{i_1 \dots i_N} \epsilon_{j_1 \dots j_N} \\ &= N(N-1) \sum_{i_1 \dots i_N j_1 \dots j_N} \delta_{i_1 k_1} \delta_{j_1 l_1} \delta_{i_2 k_2} \delta_{j_2 l_2} a_{i_3 j_3} \dots a_{i_N j_N} \\ & \quad \cdot \epsilon_{i_1 \dots i_N} \epsilon_{j_1 \dots j_N} \\ &= N(N-1) \sum_{i_3 \dots i_N j_3 \dots j_N} a_{i_3 j_3} \dots a_{i_N j_N} \\ & \quad \cdot \epsilon_{k_1 k_2 i_3 \dots i_N} \epsilon_{l_1 l_2 j_3 \dots j_N}, \end{aligned} \quad (12)$$

$$\Gamma_{i_1 j_1 i_2 j_2} = \sum_{k_1 l_1 k_2 l_2} \alpha_{k_1 i_1} \alpha_{l_1 j_1} \alpha_{k_2 i_2} \alpha_{l_2 j_2} \frac{\partial}{\partial a_{k_1 l_1}} \frac{\partial}{\partial a_{k_2 l_2}} n. \quad (13)$$

The tensor Γ would provide the reduced density matrix that we are seeking. We can use the relationship between matrix α and γ to obtain the reduced density matrix formula with the expression γ . These results appear to be similar to the expressions provided in ref.[35].

We can obtain the explicit formula of the first-order derivative of the total energy by simple differentiation with respect to parameter γ . The result is given as fol-

lows:

$$\begin{aligned}
& \frac{\partial}{\partial \gamma_{ij}^x} \gamma_{j'j}^x E^{xy} \\
= & \sum_{k_1 l_1 k_2 l_2} H_{k_1 l_1 k_2 l_2} \cdot \\
& \left(\frac{1}{2} (Q_r M \times Q_r M \times Q_r M q3 Q_l \times Q_l \times Q_l)_{j l_1 l_2 i k_2 k_1} \right. \\
& - (k_1 \leftrightarrow k_2) \\
& + \frac{1}{2} (Q_r M \times Q_r \times \gamma^x Q_r r3 Q_l \times Q_l \gamma^y \times Q_l)_{j l_1 k_2 i l_2 k_1} \\
& - ((Q_r \times \gamma^x Q_r \times Q_r M r3 Q_l \gamma^y \times Q_l \times Q_l)_{l_1 j l_2 i k_2 k_1} \\
& - (Q_r M \times Q_r \times Q_r M r3 Q_l \times Q_l \times Q_l)_{l_1 i l_2 j k_2 k_1}) \\
& - (k_1 \leftrightarrow k_2) \\
& + \frac{1}{2} (Q_r \times Q_r M \times \gamma^x Q_r r3 Q_l \gamma^y \times Q_l \times Q_l)_{l_1 j k_2 i l_2 k_1} \\
& \left. + \frac{1}{2} (Q_r \times Q_r \times \gamma^x Q_r s3 Q_l \gamma^y \times Q_l \times Q_l)_{l_1 i j l_2 k_2 k_1} \right) \quad (14)
\end{aligned}$$

Here, we are using the eigendecomposition

$$B = Q_r M Q_l, \quad (15)$$

where

$$B = -\gamma^y \gamma^x. \quad (16)$$

Tensors $q3$, $r3$, and $s3$ are rank-3 tensors defined as follows:

$$\begin{aligned}
q3_{i_1 i_2 i_3} = & ((1 + Mt)_{i_1 i_1}^{-1} (1 + Mt)_{i_2 i_2}^{-1} (1 + Mt)_{i_3 i_3}^{-1} \\
& \cdot \text{pf}(1 + Bt))|_{t^{N/2-3}}, \quad (17)
\end{aligned}$$

$$\begin{aligned}
r3_{i_1 i_2 i_3} = & ((1 + Mt)_{i_1 i_1}^{-1} (1 + Mt)_{i_2 i_2}^{-1} (1 + Mt)_{i_3 i_3}^{-1} \\
& \cdot \text{pf}(1 + Bt))|_{t^{N/2-2}}, \quad (18)
\end{aligned}$$

$$\begin{aligned}
s3_{i_1 i_2 i_3} = & ((1 + Mt)_{i_1 i_1}^{-1} (1 + Mt)_{i_2 i_2}^{-1} (1 + Mt)_{i_3 i_3}^{-1} \\
& \cdot \text{pf}(1 + Bt))|_{t^{N/2-1}}. \quad (19)
\end{aligned}$$

The above expressions show the diagonal elements of tensors $q3$, $r3$, and $s3$. In eq.(14), these tensors are used as rank-6 tensors with diagonal entries. The tensor product with the cross term is defined similar to that in ref.[36]. For example, the first line

$$(Q_r M \times Q_r M \times Q_r M q3 Q_l \times Q_l \times Q_l)_{j l_1 l_2 i k_2 k_1} \quad (20)$$

is equal to

$$\begin{aligned}
& ((B(1 + Bt)^{-1})_{ji} (B(1 + Bt)^{-1})_{l_1 k_2} (B(1 + Bt)^{-1})_{l_2 k_1} \\
& \cdot \text{pf}(1 + Bt))|_{t^{N/2-3}}. \quad (21)
\end{aligned}$$

These values for both the energy and the first-order derivatives can be obtained by operation with $O(K^2 M^5)$ steps, where K is the number of terms of the AGP states and M is the number of orbitals or the system size.

In the foregoing studies, we refer to the variation with the linear combination of AGP states as the extended symmetric tensor decomposition (ESTD). However, we prefer to call it AGP-CI hereafter, for the sake of clarity.

In the real calculation of AGP-CI, we first consider the variation independently for each geminal until the energy level of the Hartree-Fock is attained. After all of the geminals are at the Hartree-Fock level, we combine each geminal state and perform the variation for the total state.

In the expression of the first derivative, there appear rank-6 tensors, but they behave essentially as rank-3 tensors in the real calculations. The bottleneck of the total variational calculation is the product of the rank-4 tensor with rank-2 tensors. We obtained a format to perform this $O(M^5)$ operation for only four times for both the total energy and the first-order derivative using the developed method. In the future, we intend to further reduce the computational cost for this $O(M^5)$ operation.

For the AGP-CI calculation of the Hubbard model, we can use the tensor decomposition for the two-electron energy term given by

$$W_{i_1 j_1 i_2 j_2} = \sum_{i=1}^M w_{i_1}^{(1),i} w_{j_1}^{(2),i} w_{i_2}^{(3),i} w_{j_2}^{(4),i}, \quad (22)$$

where $w^{(1)}$, $w^{(2)}$, $w^{(3)}$, and $w^{(4)}$ are rank-one tensors for the Hubbard repulsion term. With this decomposition, we found that the energy variation could be performed with scaling $O(M^3)$ for the energy and $O(M^4)$ for the first derivative for both the kinetic and repulsion energy terms.

III. RESULT

We changed the variational parameters of the geminals in the AGP-CI from the real skew-symmetric matrices to complex skew-symmetric matrices. As a result, the energy obtained for the system of the water molecule with STO-3G basis set that we used in ref.[36] came closer to the exact value. Table I shows the result with complex parameters.

Method	Total energy
AGP-CI, real parameters, $K = 16$	-75.012415900
AGP-CI, complex parameters, $K = 16$	-75.012425253
Exact	-75.012425818

TABLE I: Total energy (in units of hartrees) of H_2O with STO-3G basis set obtained by AGP-CI. For comparison, the full-CI calculation was taken from ref.[36].

Here, the result with real parameters and the full-CI result was taken from ref.[36]. We observed that after changing the parameters to be complex, the resulting energy is closer to the exact energy. For this case, the resul-

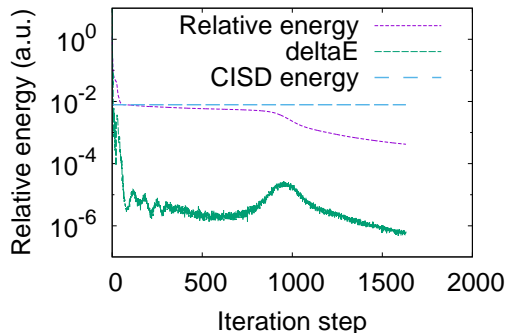


FIG. 1: The relative energy and energy changes (δE) on the variation of the water molecule with the DZ basis set. The number of AGPs (K) is set to 200.

tant energy is around 5.7×10^{-7} hartree. If we desire, we could just change the threshold value in the variational procedure and could reduce the resultant energy almost arbitrarily.

Next, we show the result for the water molecule with the Dunning double-zeta basis set, which is defined in ref.[36]. We optimized our numerical code to obtain the energy. After that, we enlarged the number of states of AGP-CI by almost threefold. Table II shows the result

Method	Total energy
Hartree-Fock	-76.00983760
AGP-CI, $K = 4$	-76.13814833
AGP-CI, $K = 60$	-76.15509884
AGP-CI, $K = 200$	-76.15771517
CISD (ref.[2])	-76.150015
CCSD (ref.[3])	-76.156078
Exact (ref.[2])	-76.157866

TABLE II: Total energy (in units of hartrees) of H_2O with the DZ basis set obtained by AGP-CI. For comparison, the full-CI result was taken from ref.[2]. The CISD result in ref.[2] and the CCSD result in ref.[3] are also included.

of AGP-CI with $K = 200$. All the other values are taken from the references mentioned above. The configuration interaction singles and doubles (CISD) and the coupled cluster singles and doubles (CCSD) results are also included from the references. For $K = 200$, the resultant energy is around 1.5×10^{-4} hartree and significantly reduced from the former result. We understand that this result satisfies the requirement of the chemical accuracy. The size of the Hilbert space of this system is approximately 1.3×10^7 ; our compact AGP states with 200 terms well capture the total wavefunction of this size. Fig.1 shows the behavior of the AGP-CI energy with respect

to the exact energy for the iteration steps. The energy change for one iteration step is also shown as δE . This graph shows the first half of the total iteration steps for this system. The energy level of CISD is also shown as a horizontal line. As can be seen from the graph, the relative energy first drops sharply and is then trapped near the CISD energy. After a long interval, the energy starts to drop again and approaches the exact value. We have not yet clarified the reason why the AGP-CI energy is trapped near the CISD energy. The reason could be that there is a large concentration of the density of states of the AGPs near the CISD energy level. We could possibly imagine that if we can construct the CISD state before AGP-CI and prepare the initial AGP-CI wavefunction as imitating the CISD wavefunction then we could improve the quality of the total variation. Moreover, we could observe the following character of AGP-CI. For this system, the number of configurations for CISD is approximately the square of the number of orbitals. Then, since the AGPs include the Slater determinants, we could obtain fairly good AGP-CI results after setting the number of states larger than the square of the number of orbitals. This would mean that the AGP-CI result is likely to behave polynomially on the computational cost. As AGP states are continuous functions rather than discrete Slater determinants, we expect good energy improvement compared with CISD.

Thirdly, we introduce the results of AGP-CI for the one-dimensional half-filled Hubbard model with 14 sites. The parameter U/t is set to 1.0. Table III shows our re-

Method	Total energy
Hartree-Fock	-14.47583682
AGP-CI, $K = 1$	-14.52254127
AGP-CI, $K = 4$	-14.63322447
AGP-CI, $K = 16$	-14.70368298
AGP-CI, $K = 100$	-14.70437808
AGP-CI, $K = 500$	-14.71456970
Exact (ref.[18])	-14.7147075

TABLE III: Total energy of the 14-site Hubbard model with $U/t=1.0$ obtained by AGP-CI. For comparison, the full-CI result of ref.[18] is also shown.

sult of AGP-CI for this system. The result with $K = 1$ is slightly below the Hartree-Fock energy. When we increase the number of states up to 500, we observe a resultant energy of 1.3×10^{-4} . We understand that this result is in good agreement with the right ground state. This size of the number of states in AGP-CI was possible to achieve after introducing the Hamiltonian decomposition for the Hubbard repulsion term. Fig.2 shows the behavior of the energy of this system on the variation process. When the variation starts, the energy is trapped on some local energy level. Then, after some interval, the energy rapidly decreases and becomes closer to the exact value. Then, the variation is almost converged. For this system

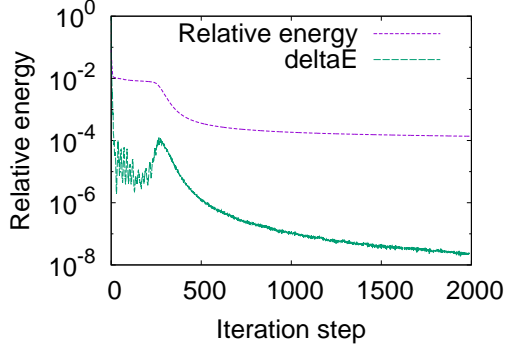


FIG. 2: The relative energy and energy changes on the variation of the one-dimensional 14-site Hubbard model with $U/t = 1.0$. The number of AGPs (K) is set to 500.

the size of the total Hilbert space is about 4.0×10^7 . The ground-state wavefunction of this large Hilbert space is well captured by 500 AGP states.

Finally, we introduce the result for the 4×4 two-dimensional half-filled Hubbard model. The parameter U/t is set to 10.0. In Table IV, we show the AGP-CI

Method	Total energy
Hartree-Fock	-6.06641304
AGP-CI, $K = 1$	-6.08549342
AGP-CI, $K = 4$	-6.46641223
AGP-CI, $K = 16$	-6.68276779
AGP-CI, $K = 100$	-6.91808110
AGP-CI, $K = 400$	-7.00753607
Exact (ref.[20])	-7.13239

TABLE IV: Total energy of the 4×4 Hubbard model with $U/t=10.0$ obtained by AGP-CI. For comparison, the full-CI result of ref.[20] is also shown.

result for this system. The energy gradually improves when the number of states increases. When $K = 400$, the resultant energy is around 0.13. This two-dimensional Hubbard model with a relatively large repulsion energy seems to be strongly correlated, and a large number of states are required for a better description of the ground state. In this system, the dimension of the total Hilbert space is approximately 6.0×10^8 , which is larger than the former systems. Fig.3 shows the behavior of the relative energy on the variation process. As we can see from the figure, the energy sharply drops down on the early stage of the variation. Then, after the energy attains a certain value, the variation converges. This system of the two-dimensional Hubbard model has a highly symmetric structure; therefore, if we could include this symmetry of the Hubbard model, the AGP-CI variation would dra-

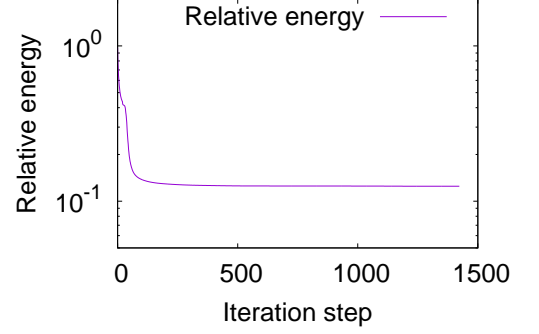


FIG. 3: The relative energy on the variation of the 4×4 Hubbard model with $U/t = 10.0$. The number of AGPs (K) is set to 400.

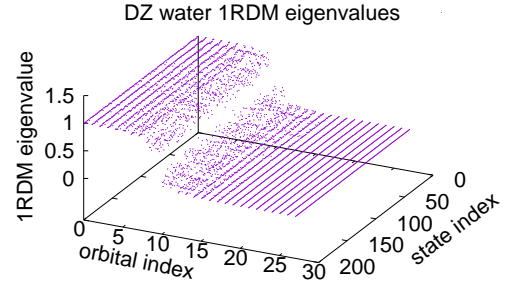


FIG. 4: 1RDM eigenvalues of the water molecule with the DZ basis set. Eigenvalues are taken for each AGP state in AGP-CI. The number of AGPs (K) is set to 200, and the number of electrons is set to 10.

matically improve.

We further analyzed the distribution of the eigenvalues of the first-order reduced density matrix (1RDM) for each AGP state in AGP-CI. Figs. 4, 5, and 6 respectively show the eigenvalue distribution for the DZ water, the one-dimensional Hubbard model, and the two-dimensional Hubbard model at the end of the variation. The horizontal plane shows the index of the AGP state and the index of the eigenvalue. The vertical axis shows the magnitude of the eigenvalue. The eigenvalue of the 1RDM corresponds to the occupation number of the natural orbital of the AGP state. These distribution of the eigenvalue does not appear on the case of Slater determinants. As we can see from these figures, the distribution of the eigenvalue has a similar shape between different geminals in each system. This is a result of the condition of the AGP state that each AGP state in AGP-CI should have energy close to the ground-state energy. The distribution of DZ water is most narrow and that

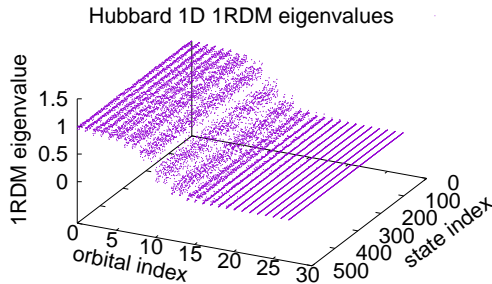


FIG. 5: 1RDM eigenvalues of the one-dimensional 14-site Hubbard model with $U/t = 1.0$. The number of AGPs (K) is set to 500, and the number of electrons is set to 14.

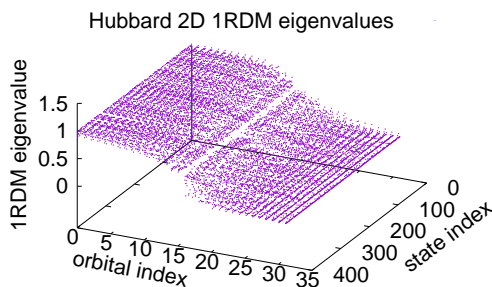


FIG. 6: 1RDM eigenvalues of the 4×4 Hubbard model with $U/t = 10.0$. The number of AGPs (K) is set to 400, and the number of electrons is set to 16.

of the two-dimensional Hubbard model is most broad in these three cases. The broadness of these distributions might be reflecting the strength of the electronic correlation of each system. Therefore, we can assume that the requirement for a larger number of states for the two-dimensional Hubbard model is a result of the stronger electronic correlation. Since these distributions are simi-

lar for each AGP state, we can assume that the required geminals in AGP-CI are distributing across a restricted area of the geminal space characterized by each system. It would benefit the whole calculation if we successfully characterize the nature of the geminals mentioned above. This could be done with a well-organized control of the eigenvalues of each geminal matrix.

IV. CONCLUSION

We tested the AGP-CI formalism on a double-zeta water molecule and Hubbard models with an extended number of sites. The results for the water molecule and 14-site Hubbard model were very close to the exact result. From this, we conclude that the required number of states for AGP-CI increases only moderately with the problem size. The calculation on the Hubbard model was based on the tensor decomposition for the two-electron part of the Hamiltonian. We could also use this tensor decomposition for molecular systems and could possibly reduce the computational scaling by one order.[38] There are non-trivial relationships of the AGP-CI energy with the CISD energy. If we could use the CISD wavefunctions before the AGP-CI calculation, we would expect that the total variation process would become shorter. In the future, we will further study the dependence of the required number of AGP states on the size of the problem. If we could utilize tensor decomposition for the Hamiltonian, we could investigate the behavior of AGP-CI for larger systems. With an analysis of the nature of the geminal states appearing in AGP-CI, we can improve the whole variation process. We only used dozens of CPUs for the above calculations; however, if this is extended to larger computing resources, we can perform the AGP-CI calculation with more extended systems.

Acknowledgment

We acknowledge the Strategic Programs for Innovative Research by MEXT and “Priority Issue on Post-K Computer” (Development of new fundamental technologies for high-efficiency energy creation, conversion or storage, and use) for financial support during our research. Some of the computations in the present study were performed at the Institute for Molecular Science, Okazaki, Japan.

-
- [1] I. Shavitt, Mol. Phys. 94, 3 (1998).
 - [2] P. Saxe, H. F. Schaefer, and N. C. Handy, Chem. Phys. Lett. 79, 202 (1981).
 - [3] G. D. Purvis and R. J. Bartlett, J. Chem. Phys. 76, 1910(1982).
 - [4] H. Werner and P. J. Knowles, J. Chem. Phys. 89, 5803 (1988).
 - [5] N. Oliphant and L. Adamowicz, J. Chem. Phys. 94, 1229 (1991).
 - [6] F. A. Evangelista, J. Chem. Phys. 149, 030901 (2018).
 - [7] P. Hohenberg and W. Kohn, Phys. Rev. 136, B864 (1964).
 - [8] W. Kohn and L. J. Sham, Phys. Rev. 140, A1133 (1965).
 - [9] M. Levy, Phys. Rev. A 26, 1200 (1982).

- [10] W. M. C. Foulkes, L. Mitas, R. J. Needs, and G. Rajagopal, *Rev. Mod. Phys.* 73, 33 (2001).
- [11] M. Bajdich, L. Mitas, G. Drobný, L. K. Wagner, and K. E. Schmidt, *Phys. Rev. Lett.* 96, 130201 (2006).
- [12] M. Bajdich, L. Mitas, L. K. Wagner, and K. E. Schmidt, *Phys. Rev. B* 77, 115112 (2008).
- [13] E. Neuscamman, *Phys. Rev. Lett.* 109, 203001 (2012).
- [14] E. Neuscamman, *J. Chem. Phys.* 139, 194105 (2013).
- [15] A. Zen, E. Coccia, Y. Luo, S. Sorella, and L. Guidoni, *J. Chem. Theory Comput.* 10 (3), 1048 (2014).
- [16] Y. Luo, A. Zen, and S. Sorella, *J. Chem. Phys.* 141, 194112 (2014).
- [17] A. Zen, Y. Luo, G. Mazzola, L. Guidoni, and S. Sorella, *J. Chem. Phys.* 142, 144111 (2015).
- [18] N. S. Blunt, S. D. Smart, G. H. Booth, and A. Alavi, *J. Chem. Phys.* 143, 134117 (2015).
- [19] H. Shi and S. Zhang, *Phys. Rev. B* 95, 045144 (2017).
- [20] D. Tahara and M. Imada, *J. Phys. Soc. Jpn.* 77, 114701 (2008).
- [21] A. Ikawa, S. Yamamoto, and H. Fukutome, *J. Phys. Soc. Jpn.* 62, 1653 (1993).
- [22] N. Tomita, *Phys. Rev. B* 69, 045110 (2004).
- [23] N. Tomita, *Phys. Rev. B* 79, 075113 (2009).
- [24] S. Watanabe, M. Katoh, and N. Tomita, *J. Phys. Soc. Jpn.* 82, 044705 (2013).
- [25] R. Rodriguez-Guzman, C. A. Jimenez-Hoyos, R. Schutski, and G. E. Scuseria, *Phys. Rev. B* 87, 235129 (2013).
- [26] C. A. Jimenez-Hoyos, R. Rodriguez-Guzman, and G. E. Scuseria, *J. Chem. Phys.* 139, 204102 (2013).
- [27] R. Rodriguez-Guzman, C. A. Jimenez-Hoyos, and G. E. Scuseria, *Phys. Rev. B* 90, 195110 (2014).
- [28] A. J. Coleman, *Rev. Mod. Phys.* 35, 668 (1963).
- [29] A. J. Coleman, *J. Math. Phys.* 6, 1425 (1965).
- [30] J. V. Ortiz, B. Weiner, and Y. Ohn, *Int. J. Quantum Chem.* 20, 113 (1981).
- [31] B. Weiner and J. V. Ortiz, *J. Chem. Phys.* 117, 5135 (2002).
- [32] S. Giorgini, L. P. Pitaevskii, and S. Stringari, *Rev. Mod. Phys.* 80, 1215-1274 (2008).
- [33] V. N. Staroverov and G. E. Scuseria, *J. Chem. Phys.* 117, 11107 (2002).
- [34] G. E. Scuseria, C. A. Jimenez-Hoyos, T. M. Henderson, K. Samanta, and J. K. Ellis, *J. Chem. Phys.* 135, 124108 (2011).
- [35] W. Uemura, S. Kasamatsu, and O. Sugino, *Phys. Rev. A* 91, 062504 (2015).
- [36] W. Uemura and T. Nakajima, *Phys. Rev. A* 99, 012519 (2019).
- [37] T. Mizusaki, M. Oi, and N. Shimizu, *Phys. Lett. B* 779, 237(2018).
- [38] U. Benedikt, A. A. Auer, M. Espig, and W. Hackbusch, *J. Chem. Phys.* 134, 054118 (2011).